Automatica 48 (2012) 2686–2692

Contents lists available at SciVerse ScienceDirect

Automatica

journal homepage: www.elsevier.com/locate/automatica

Brief paper

Integrated guidance and control for dual-control missiles based on small-gain theorem☆

Han Yan [1], Haibo Ji

University of Science and Technology of China, Hefei, Anhui 230027, PR China

ARTICLE INFO

Article history:
Received 31 March 2011
Received in revised form
17 April 2012
Accepted 31 May 2012
Available online 21 July 2012

Keywords:
Integrated guidance and control
Small-gain theorem
Input-to-state stability
Robustness

ABSTRACT

An integrated guidance and control (IGC) design approach is proposed based on small-gain theorem for missiles steered by both canard and tail controls. The angle of attack and pitch rate commands, which are aimed at producing desired aerodynamic lift to achieve robust tracking of a maneuvering target, are generated by a guidance law that is designed using input-to-state stability (ISS) theory. An IGC law is developed utilizing generalized small-gain theorem to enforce the commands, and it can be shown that both the line-of-sight (LOS) rate and the tracking error are input-to-state practically stable (ISpS) with respect to target maneuvers and missile model uncertainties. The algorithm is tested using computer simulations against a maneuvering target.

1. Introduction

The guidance and control systems of interceptor missiles are usually designed separately and then integrated, but it can be argued that this scheme cannot fully exploit synergistic relationships between the two subsystems or strictly maintain the stability of the overall system. In particular, as the relative range between interceptor and target becomes small, rapid changes in the relative geometry might cause the separation design method to be invalid (Shima, Idan, & Golan, 2006). Integrated guidance and control (IGC) design is one of emerging trends in missile control technology, because it can improve the performance of interceptors by viewing guidance and control loops as an integrated system and taking couplings between subsystems into account. Such a design can reduce the cost of the required sensors and increase the system reliability (Williams, Richman, & Friedland, 1983). Since the canard fins can generate an aerodynamic force to drive the missiles to the required direction, a canard configuration was employed in some short-range air-to-air missiles (Shima et al., 2006). However, canard control has its limit due to aerodynamic saturation at high angles of attack, especially for long fuselage missiles, and a tail control is often preferred. Therefore, some researchers proposed IGC approaches by using both canard and tail controls to obtain better performance for dual-control missiles (Idan, Shima, & Golan, 2007).

After IGC design was put forward in Williams et al. (1983), various control methods have been introduced. Suboptimal control methods were introduced to solve IGC problem in three dimensions (Menon & Ohlmeyer, 1999; Palumbo & Jackson, 1999; Xin, Balakrishnan, & Ohlmeyer, 2006). The state dependent Riccati equation (SDRE) technique was employed in Menon and Ohlmeyer (1999) based on a six-degrees-of-freedom (6-DOF) nonlinear missile model for IGC design with the assumption that the target velocity can be negligible when compared with the missile velocity. Palumbo and Jackson (1999) formulated the IGC problem as a single minmax optimization problem when the target acceleration was known as a priori to find a controller that minimizes the final miss distance and control energy, in which the SDRE technique was employed to handle this finite-time horizon nonlinear problem. However, as mentioned in that paper, since solving SDRE online is time consuming, it may be not feasible for a 6-DOF missile system. Xin and co-workers (Xin et al., 2006) solved the nonlinear infinite-horizon IGC problem by utilizing $\theta - D$ technique. Their method gave an approximate closed-form suboptimal feedback controller with no iterative solutions as in the case of the SDRE approach, but the disturbances and uncertainties of the 6-DOF missile model were not considered.

Sliding-mode control (SMC) is another typical method that is utilized to design IGC algorithm in pitch channel (Idan et al., 2007; Shima et al., 2006; Shtessel, Shkolnikov, & Levant, 2009; Shtessel & Tournes, 2009), especially for dual-control missiles (Idan et al., 2007; Shtessel & Tournes, 2009). In Shtessel et al.

☆ This work was supported by the National Natural Science Foundation of China under Grant 60674029 and the USTC Special Grant for Postgraduate Research, Innovation and Practice. The material in this paper was not presented at any conference. This paper was recommended for publication in revised form by Associate Editor C.C. Cheah under the direction of Editor Toshiharu Sugie.

E-mail addresses: yanhan@mail.ustc.edu.cn (H. Yan), jihb@ustc.edu.cn (H. Ji).

[1] Tel.: +86 0551 3601521; fax: +86 0551 3603244.

0005-1098/$ – see front matter © 2012 Elsevier Ltd. All rights reserved.
doi:10.1016/j.automatica.2012.06.084

(2009), a sliding surface that depends on the line-of-sight (LOS) rate was defined in the guidance loop with the missile pitch rate viewed as a virtual control. In the control loop, the second-order SMC was used to control the pitch rate to track the virtual control robustly in finite time. Shima and co-workers (Shima et al., 2006) used SMC to obtain IGC design by using zero-effort miss (ZEM) distance as a single sliding surface with the assumption that the target acceleration can be measured. For missiles with both canard and tail controls, they chose an additional sliding surface based on flight-control considerations that can achieve improved stability and shaped/damped response (Idan et al., 2007). Note that, in order to remove nonlinear terms, the equations of IGC model in Idan et al. (2007) and Shima et al. (2006) were formulated under the assumption that the angle between LOS and missile velocity is almost constant, but this assumption might be not proper in practice since large maneuvers of a target may lead to significant variation of that angle. In Shtessel and Tournes (2009), an IGC algorithm, integrated with the smooth second-order sliding mode guidance law in Shtessel, Shkolnikov, and Levant (2007), was developed using higher-order SMC for interceptors steered by a combination of aerodynamic lift, sustainer thrust, and center-of-gravity divert thrusters. With this approach, a fast tracking of the attitude command can be achieved, however, it may not strictly maintain the stability of the overall system during the process of tracking commands in each channel. Backstepping scheme was also used to design IGC algorithm in the pitch channel in Sharma and Richards (2004) by linearizing the missile dynamics and neglecting the lift contribution of control surfaces based on the assumption that the neural network can provide accurate estimates of uncertainties.

Besides the works mentioned above, the feedback linearization method (Menon & Ohlmeyer, 2001), subspace stabilization strategy (Tournes & Wilkerson, 2001) and some other control methods were also utilized in the IGC design problem. These researches made great contributions to the development of IGC design, but many existing results were obtained based on some strong assumptions or without considering robustness against uncertainties and disturbances.

In this paper, a novel IGC design approach, against maneuvering targets, is proposed using small-gain theorem (Jiang, Teel, & Praly, 1994) and input-to-state stability (ISS) (Sontag, 1989) for missiles controlled by forward and aft control surfaces. An ISS-based guidance law is designed for target interception meaning that the law keeps the LOS rate within a small neighborhood of zero in the presence of unknown target maneuvers. Then, an IGC law is developed utilizing small-gain theorem to control angle of attack and pitch rate to track commands generated by an inversion depending on the ISS-based guidance law. Theoretical analysis shows that the IGC approach makes both the LOS rate and the tracking error of attitude angle (rate) be input-to-state practically stable (ISpS) with respect to target maneuvers and missile model uncertainties which are not needed to be known as a priori. It is worth claiming that our approach is formulated without the assumption that the angle between LOS and missile velocity is almost constant, and the lift contribution of control surfaces is also taken into account. Besides that, the stability of the overall system can be guaranteed by small-gain theorem.

2. Model derivation

2.1. Engagement kinematics

The corresponding equations of motion between missile and target are given by Zhou, Sun, and Teo (2009)

$$\dot{R} = V_T\cos(q-\varphi_T) - V_M\cos(q-\varphi_M) \tag{1a}$$

$$R\dot{q} = -V_T\sin(q-\varphi_T) + V_M\sin(q-\varphi_M) \tag{1b}$$

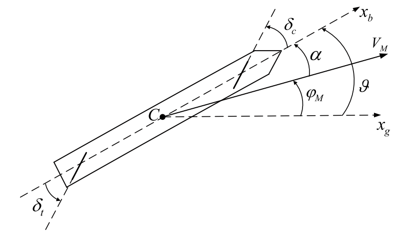

Fig. 1. Planar interception geometry.

where R is relative range; q is line-of-sight angle; φ_M and φ_T are missile and target fight path angles, respectively; and V_M and V_T are missile and target velocity, respectively. Suppose that the missile speed is constant during the end game, and the missile acceleration can be calculated as

$$a_M = V_M\dot{\varphi}_M. \tag{2}$$

Differentiating equation (1b), we have

$$\dot{\omega}_q = -2\frac{V_R}{R}\omega_q + \frac{a_{T_q}}{R} - \cos(q-\varphi_M)\frac{a_M}{R} \tag{3}$$

where $V_R = \dot{R}$, $\omega_q = \dot{q}$, and a_{T_q} is the projection of bounded target acceleration orthogonal to the LOS. It is rational to assume that $V_M > V_T$ and $|q-\varphi_M| < \frac{\pi}{2}$ when homing guidance begins, and because a guidance law should nullify the LOS rate, $|q-\varphi_M| < \frac{\pi}{2}$ will hold generally in the whole process of homing guidance, that is, there exists a positive real number of κ such that $\cos(q-\varphi_M) \geq \kappa$.

2.2. Missile dynamics

Fig. 1 gives the missile planar dynamics, where C is the missile's center of gravity, Cx_b is aligned with the missile's longitudinal axis, and Cx_g is parallel to the horizontal. The planar missile dynamics with both canard and tail controls are given by Idan et al. (2007)

$$J\dot{\omega} = M(\alpha,\omega,\delta_c,\delta_t) \tag{4a}$$

$$\dot{\vartheta} = \omega \tag{4b}$$

$$\dot{\varphi}_M = \frac{L(\alpha,\delta_c,\delta_t)}{mV_M} \tag{4c}$$

$$\alpha = \vartheta - \varphi_M \tag{4d}$$

$$\dot{\delta}_c = \frac{\delta_c^c-\delta_c}{\tau_c}, \qquad \dot{\delta}_t = \frac{\delta_t^c-\delta_t}{\tau_t} \tag{4e}$$

where J is moment of inertia; ω is pitch rate; ϑ is pitch angle; m is missile mass; α is angle of attack; δ_c and δ_t are canard and tail controls, respectively; and L and M are, respectively, aerodynamic forces and moments, which are nonlinear functions of the related variables, in particular α, ω, δ_c, and δ_t. It is assumed that the missile actuators follow first-order dynamics with time constants τ_c and τ_t as expressed by Eq. (4e). When α, ω, δ_c, and δ_t are in relatively small domains around zero, Eqs. (4) can be transformed into a linearized short-period form (Idan et al., 2007; Sharma & Richards, 2004; Shima et al., 2006; Wise & Broy, 1998), that is,

$$\dot{\alpha} = \omega - \frac{l_\alpha}{V_M}\alpha - \frac{l_{\delta_c}}{V_M}\delta_c - \frac{l_{\delta_t}}{V_M}\delta_t + \Delta_\alpha \tag{5a}$$

$$\dot{\vartheta} = \omega \tag{5b}$$

$$\dot{\omega} = m_\alpha\alpha + m_\omega\omega + m_{\delta_c}\delta_c + m_{\delta_t}\delta_t + \Delta_\omega \tag{5c}$$

$$\alpha = \vartheta - \varphi_M \tag{5d}$$

$$\dot{\delta}_c = \frac{\delta_c^c-\delta_c}{\tau_c}, \qquad \dot{\delta}_t = \frac{\delta_t^c-\delta_t}{\tau_t} \tag{5e}$$

with $l_x = \frac{\partial(L/m)}{\partial x}$, $m_x = \frac{\partial(M/J)}{\partial x}$, and Δ_α and Δ_ω are bounded uncertainties.

3. Integrated guidance and control law design

3.1. Concepts and preliminaries

Consider the following general interconnected system

$$H_1: \dot{x}_1 = f_1(x_1, y_2, u_1), \qquad y_1 = h_1(x_1, y_2, u_1) \tag{6}$$

$$H_2: \dot{x}_2 = f_2(x_2, y_1, u_2), \qquad y_2 = h_2(x_2, y_1, u_2) \tag{7}$$

where, for $i = 1, 2$, $x_i \in \mathbb{R}^{n_i}$, $u_i \in \mathbb{R}^{m_i}$, and $y_i \in \mathbb{R}^{p_i}$. The functions f_1, f_2, h_1 and h_2 are smooth and a smooth function h exists such that

$$(y_1, y_2) = h(x_1, x_2, u_1, u_2)$$

is the unique solution of

$$\begin{cases} y_1 = h_1(x_1, h_2(x_2, y_1, u_2), u_1) \\ y_2 = h_2(x_2, h_1(x_1, y_2, u_1), u_2). \end{cases}$$

We have

Theorem 1 (Jiang et al., 1994)**.** *Suppose (6) and (7) are ISS with (y_2, u_1) (respectively (y_1, u_2)) as input, y_1 (respectively y_2) as output, and there exist class $\mathcal{KL}$ functions β_1, β_2, class $\mathcal{K}$ functions $\gamma_1^y, \gamma_1^u, \gamma_2^y, \gamma_2^u$, and nonnegative constants d_1, d_2 such that*

$$\|y_1(t)\| \le \beta_1(\|x_1(0)\|, t) + \gamma_1^y(\|y_{2t}\|) + \gamma_1^u(\|u_1\|) + d_1 \tag{8a}$$

$$\|y_2(t)\| \le \beta_2(\|x_2(0)\|, t) + \gamma_2^y(\|y_{1t}\|) + \gamma_2^u(\|u_2\|) + d_2. \tag{8b}$$

If two class $\mathcal{K}_\infty$ functions ρ_1 and ρ_2 and a nonnegative real number s_l satisfying

$$\begin{cases} (Id + \rho_2) \circ \gamma_2^y \circ (Id + \rho_1) \circ \gamma_1^y(s) \le s \\ (Id + \rho_1) \circ \gamma_1^y \circ (Id + \rho_2) \circ \gamma_2^y(s) \le s \end{cases}, \quad \forall s \ge s_l \tag{9}$$

exist, where Id denotes the identity function and $\circ$ is composition of functions, system (6)–(7) with $u = (u_1, u_2)$ as input, $y = (y_1, y_2)$ as output and $x = (x_1, x_2)$ as state will be input-to-output practically stable (IOpS) (input-to-output stable (IOS) if $s_l = d_1 = d_2 = 0$).

3.2. ISS-based guidance law design

Accepting the intuition that zeroing the LOS rate will lead to interception, we will design a guidance law to keep the LOS rate within a small neighborhood of zero in this section.

Theorem 2. *In the interception of a maneuvering target, assume that the inequality $\cos(q - \varphi_M) \ge \kappa$ (κ is a positive real number) holds in a reasonable flight domain. Then the closed-loop system of system (3) and guidance law*

$$a_M = a_M^* = \frac{1}{\cos(q - \varphi_M)}\left(R\left(K + \frac{1}{2\xi^2}\right)\omega_q - 2V_R\omega_q\right) \tag{10}$$

is ISS with respect to the target maneuvers for $K > 0$ and $\xi > 0$, that is,

$$|\omega_q(t)| \le e^{-Kt}|\omega_q(0)| + \frac{\xi}{\sqrt{2K}R_m}\sqrt{1 - e^{-2Kt}} \sup_{0\le\tau\le t} |a_{T_q}(\tau)|. \tag{11}$$

Moreover, if the target normal acceleration vanishes, the origin of the closed-loop system will be exponentially stable.

Proof. The derivative of $V = \frac{1}{2}\omega_q^2$ along the trajectories of system (3) is given by

$$\dot{V} = \omega_q\left(-2\frac{V_R}{R}\omega_q + \frac{a_{T_q}}{R} - \cos(q - \varphi_M)\frac{a_M}{R}\right). \tag{12}$$

Applying

$$\omega_q \frac{a_{T_q}}{R} \le \frac{1}{2\xi^2}\omega_q^2 + \frac{\xi^2}{2}\frac{a_{T_q}^2}{R^2} \tag{13}$$

where $\xi > 0$, into Eq. (12), we obtain

$$\dot{V} \le \omega_q\left(-2\frac{V_R}{R}\omega_q + \frac{\omega_q}{2\xi^2} - \cos(q - \varphi_M)\frac{a_M}{R}\right) + \frac{\xi^2}{2}\frac{a_{T_q}^2}{R^2}. \tag{14}$$

Substituting (10) into Eq. (14) yields

$$\dot{V} \le -K\omega_q^2 + \frac{\xi^2}{2}\frac{a_{T_q}^2}{R^2}. \tag{15}$$

In the interception endgame, inequality $0 < R_m \le R \le R_M$ holds. Hence,

$$\dot{V} \le -K\omega_q^2 + \frac{\xi^2}{2}\frac{a_{T_q}^2}{R_m^2} \le -2KV + \frac{\xi^2}{2}\frac{a_{T_q}^2}{R_m^2}. \tag{16}$$

Solving the differential inequality (16) yields

$$V(\omega_q(t)) \le e^{-2Kt}V(\omega_q(0)) + \frac{\xi^2}{4KR_m^2}\left(1 - e^{-2Kt}\right) \times \sup_{0\le\tau\le t} a_{T_q}^2(\tau). \tag{17}$$

Taking the square roots and using the inequality $\sqrt{a^2 + b^2} \le a + b$ for nonnegative numbers a and b, we can see that Eq. (11) holds. Therefore, the closed-loop system of system (3) and guidance law (10) is ISS with respect to the target maneuvers.

Moreover, if the target normal acceleration vanishes, that is, $a_{T_q} = 0$, Eq. (11) can be rewritten as $|\omega_q(t)| \le e^{-Kt}|\omega_q(0)|$. In this case, the origin of the closed-loop system is exponentially stable. $\square$

Remark 1. In guidance law (10), $-2V_R\omega_q$ stands for realistic true proportional navigation (RTPN) guidance (Yang & Yang, 1997). That is, our guidance law is composed of a RTPN term and the term $R\omega_q$ with guidance coefficients K and ξ.

Theorem 2 shows that, with the guidance law (10), the LOS rate ω_q converges to a small neighborhood of zero by adjusting coefficients ξ and K, even though the unknown target normal acceleration exists. As R becomes small, some smaller ξ or larger K is required to keep $|\omega_q|$ in a desired domain as implied by Eq. (15), i.e., a large control energy is needed to suppress the target maneuvers, since $R = 0$ is a singular point of system (3). However, due to the finite size of missiles and targets, a successful interception can be achieved as long as the missile can supply enough control energy until R decreases to a particular intercept value in the whole process of homing guidance (Shtessel et al., 2009; Shtessel & Tournes, 2009).

3.3. IGC law design

Since the angle of attack must be kept in a reasonable domain during the end game, the command profile α^* can be chosen as a predetermined bounded smooth function. Taking the derivative of a_M^* (see Appendix) yields

$$\dot{a}_M^* = \varrho - \frac{2a_{T_R}\omega_q}{\cos(q - \varphi_M)} + \frac{\Gamma a_{T_q}}{R\cos(q - \varphi_M)} \tag{18}$$

where $\Gamma = R(K + \frac{1}{2\xi^2}) - 2V_R$, a_{T_R} is the projection of target acceleration along the LOS, and ϱ is given by

$$\begin{aligned}\varrho = {} & \frac{\sin(q-\varphi_M)}{\cos^2(q-\varphi_M)}\left(\omega_q - \frac{a_M}{V_M}\right)\Gamma\omega_q + \frac{\omega_q}{\cos(q-\varphi_M)} \\ & \times \left(\left(K + \frac{1}{2\xi^2}\right)V_R - 2R\omega_q^2 + 2\sin(q-\varphi_M)a_M\right) \\ & + \frac{\Gamma}{\cos(q-\varphi_M)}\left(-\frac{2V_R}{R}\omega_q - \cos(q-\varphi_M)\frac{a_M}{R}\right) \end{aligned} \tag{19}$$

where all the state variables including missile acceleration are assumed to be measurable. Thus, according to Eqs. (2) and (4d), we define pitch rate command ω^* and its derivative command $\dot{\omega}^*$ as

$$\omega^* = \dot{\alpha}^* + \frac{a_M^*}{V_M}, \qquad \dot{\omega}^* = \ddot{\alpha}^* + \frac{\varrho}{V_M}. \tag{20}$$

It can be seen that if command profiles $\dot{\alpha}^*$ and ω^* are enforced by control surfaces, the LOS rate will be ISS against the target maneuvers according to Theorem 2. Therefore, we will design a control law to drive α and ω to track their commands.

From Eqs. (4), we have

$$\ddot{\alpha} = A_\alpha\alpha + A_\omega\omega + A_{\delta_c}\delta_c + A_{\delta_t}\delta_t - A_{\delta_c^c}\delta_c^c - A_{\delta_t^c}\delta_t^c + \Delta_A \tag{21a}$$

$$\ddot{\omega} = B_\alpha\alpha + B_\omega\omega + B_{\delta_c}\delta_c + B_{\delta_t}\delta_t + B_{\delta_c^c}\delta_c^c + B_{\delta_t^c}\delta_t^c + \Delta_B \tag{21b}$$

where $A_\alpha = m_\alpha + \frac{l_\alpha^2}{V_M^2} - \frac{\dot{l}_\alpha}{V_M}$, $A_\omega = m_\omega - \frac{l_\alpha}{V_M}$, $A_{\delta_c} = m_{\delta_c} + \frac{l_\alpha l_{\delta_c}}{V_M^2} + \frac{l_{\delta_c}}{V_M\tau_c} - \frac{\dot{l}_{\delta_c}}{V_M}$, $A_{\delta_c^c} = \frac{l_{\delta_c}}{V_M\tau_c}$, $A_{\delta_t} = m_{\delta_t} + \frac{l_\alpha L_{\delta_t}}{V_M^2} + \frac{l_{\delta_t}}{V_M\tau_t} - \frac{\dot{l}_{\delta_t}}{V_M}$, $A_{\delta_t^c} = \frac{l_{\delta_t}}{V_M\tau_t}$, $B_\alpha = \dot{m}_\alpha + m_\omega m_\alpha - m_\alpha\frac{L_\alpha}{V_M}$, $B_\omega = \dot{m}_\omega + m_\alpha + m_\omega^2$, $B_{\delta_c} = \dot{m}_{\delta_c} + m_\omega m_{\delta_c} - m_\alpha\frac{L_{\delta_c}}{V_M} - \frac{m_{\delta_c}}{\tau_c}$, $B_{\delta_c^c} = \frac{m_{\delta_c}}{\tau_c}$, $B_{\delta_t} = \dot{m}_{\delta_t} + m_\omega m_{\delta_t} - m_\alpha\frac{L_{\delta_t}}{V_M} - \frac{m_{\delta_t}}{\tau_t}$, $B_{\delta_t^c} = \frac{m_{\delta_t}}{\tau_t}$, $\Delta_A = \Delta_\omega - \frac{L_\alpha}{V}\Delta_\alpha + \dot{\Delta}_\alpha$, $\Delta_B = m_\alpha\Delta_\alpha + m_\omega\Delta_\omega + \dot{\Delta}_\omega$. Denoting $x = [\alpha, \dot{\alpha}, \omega, \dot{\omega}]^T$, on account of Eqs. (2), (3) and (21), we obtain

$$\dot{\omega}_q = -2\frac{V_R}{R}\omega_q - \frac{\cos(q-\varphi_M)V_M}{R}c_0x + \frac{a_{T_q}}{R} \tag{22a}$$

$$\begin{aligned}\dot{x} = {} & \begin{bmatrix} 0 & 1 & 0 & 0 \\ A_\alpha & 0 & A_\omega & 0 \\ 0 & 0 & 0 & 1 \\ B_\alpha & 0 & B_\omega & 0 \end{bmatrix} x + \begin{bmatrix} 0 & 0 \\ A_{\delta_c} & A_{\delta_t} \\ 0 & 0 \\ B_{\delta_c} & B_{\delta_t} \end{bmatrix}\begin{bmatrix}\delta_c \\ \delta_t\end{bmatrix} \\ & + \begin{bmatrix} 0 & 0 \\ -A_{\delta_c^c} & -A_{\delta_t^c} \\ 0 & 0 \\ B_{\delta_c^c} & B_{\delta_t^c} \end{bmatrix}\begin{bmatrix}\delta_c^c \\ \delta_t^c\end{bmatrix} + \begin{bmatrix} 0 \\ \Delta_A \\ 0 \\ \Delta_B \end{bmatrix} \end{aligned} \tag{22b}$$

where $c_0 = \begin{bmatrix} 0 & -1 & 1 & 0 \end{bmatrix}$. By choosing

$$\begin{bmatrix}\delta_c^c \\ \delta_t^c\end{bmatrix} = E\begin{bmatrix}\delta_c \\ \delta_t\end{bmatrix} + \begin{bmatrix}u_1 \\ u_2\end{bmatrix} \tag{23}$$

with $E = \begin{bmatrix} \frac{A_{\delta_c}B_{\delta_t^c} + A_{\delta_t^c}B_{\delta_c}}{A_{\delta_c^c}B_{\delta_t^c} - A_{\delta_t^c}B_{\delta_c^c}} & \frac{A_{\delta_t}B_{\delta_t^c} + A_{\delta_t^c}B_{\delta_t}}{A_{\delta_c^c}B_{\delta_t^c} - A_{\delta_t^c}B_{\delta_c^c}} \\ \frac{B_{\delta_c^c}A_{\delta_c} + A_{\delta_c^c}B_{\delta_c}}{A_{\delta_t^c}B_{\delta_c^c} - A_{\delta_c^c}B_{\delta_t^c}} & \frac{A_{\delta_c^c}B_{\delta_t} + A_{\delta_t}B_{\delta_c^c}}{A_{\delta_t^c}B_{\delta_c^c} - A_{\delta_c^c}B_{\delta_t^c}} \end{bmatrix}$, Eq. (22) can be transformed to

$$\dot{\omega}_q = -2\frac{V_R}{R}\omega_q - \frac{\cos(q-\varphi_M)V_M}{R}c_0x + \frac{a_{T_q}}{R} \tag{24a}$$

$$\dot{x} = Ax + Bu + F\Delta \tag{24b}$$

where the matrices A, B, F, and Δ are given by

$$A = \begin{bmatrix} 0 & 1 & 0 & 0 \\ A_\alpha & 0 & A_\omega & 0 \\ 0 & 0 & 0 & 1 \\ B_\alpha & 0 & B_\omega & 0 \end{bmatrix}, \qquad B = \begin{bmatrix} 0 & 0 \\ -A_{\delta_c^c} & -A_{\delta_t^c} \\ 0 & 0 \\ B_{\delta_c^c} & B_{\delta_t^c} \end{bmatrix},$$

$$F = \begin{bmatrix} 0 & 1 & 0 & 0 \\ 0 & 0 & 0 & 1 \end{bmatrix}^T, \qquad \Delta = \begin{bmatrix}\Delta_A \\ \Delta_B\end{bmatrix}.$$

Let $x^* = [\alpha^*, \dot{\alpha}^*, \omega^*, \dot{\omega}^*]^T$, the change of variables

$$\eta = x - x^* \tag{25}$$

brings Eqs. (24) into the form

$$\begin{aligned}\dot{\omega}_q = {} & -2\frac{V_R}{R}\omega_q - \frac{\cos(q-\varphi_M)a_M^*}{R} \\ & - \frac{\cos(q-\varphi_M)V_M}{R}c_0\eta + \frac{a_{T_q}}{R}\dot{\eta} \end{aligned} \tag{26a}$$

$$\dot{\eta} = A\eta + Bu + Ax^* - \dot{x}^* + F\Delta. \tag{26b}$$

It is not difficult to see that the system can be represented in the form of (6)–(7) with H_1 defined by

$$\begin{cases} \dot{\omega}_q = -2\frac{V_R}{R}\omega_q - \frac{\cos(q-\varphi_M)a_M^*}{R} + \frac{v_1}{R} \\ \quad + \frac{\cos(q-\varphi_M)V_M}{R}y_2 \\ y_1 = \begin{bmatrix} A_\alpha\alpha^* + A_\omega\omega^* - \ddot{\alpha}^* \\ B_\alpha\alpha^* + B_\omega\omega^* - \ddot{\omega}^* \end{bmatrix}. \end{cases} \tag{27}$$

H_2 defined by

$$\begin{cases} \dot{\eta} = A\eta + Bu + Fv_2 + Fy_1 \\ y_2 = -c_0\eta \end{cases} \tag{28}$$

and

$$v_1 = a_{T_q}, \qquad v_2 = \Delta.$$

As a result of Theorem 2, system H_1 is ISS against v_1 and y_2, and the following inequality holds,

$$\begin{aligned}|\omega_q(t)| \le {} & \frac{\xi}{\sqrt{2KR_m}}\sqrt{1-e^{-2Kt}}\sup_{0\le\tau\le t}|v_1(\tau)| \\ & + \frac{\xi V_M}{\sqrt{2KR_m}}\sqrt{1-e^{-2Kt}}\sup_{0\le\tau\le t}|y_2(\tau)| + e^{-Kt}|\omega_q(0)| \\ \triangleq {} & \alpha_0\left(\sup_{0\le\tau\le t}|v_1(\tau)|\right) + \alpha_0\left(\sup_{0\le\tau\le t}|y_2(\tau)|\right) \\ & + \beta_0(|\omega_q(0)|, t). \end{aligned} \tag{29}$$

Hence, according to Proposition 3.1 of Jiang et al. (1994), for the output function y_1, the inequality

$$\begin{aligned}\|y_1\| \le {} & \gamma_1^v\left(\sup_{0\le\tau\le t}|v_1(\tau)|\right) + \gamma_1^y\left(\sup_{0\le\tau\le t}|y_2(\tau)|\right) \\ & + \beta_1(|\omega_q(0)|, t) + d_y^1 \end{aligned} \tag{30}$$

holds for a pair of class $\mathcal{K}$ functions (γ_1^v, γ_1^y), a class $\mathcal{KL}$ function β_1, and a nonnegative constant d_y^1. The main results are stated in the following theorem.

Theorem 3. *Consider the interconnected system (27) and (28). Take control law (31) as shown in Box I for $a > 0$, $b > 0$, and ε is a positive constant to be specified. If $\|\Delta\|$ is bounded, there exists $\varepsilon^* > 0$ such that system (27) is ISpS with respect to inputs v_1 and v_2 for $0 < \varepsilon \le \varepsilon^*$.*

Proof. Substituting control law (31) and the new variables

$$\widetilde{\eta}_1 = \frac{\eta_1}{\varepsilon}, \qquad \widetilde{\eta}_2 = \eta_2, \qquad \widetilde{\eta}_3 = \frac{\eta_3}{\varepsilon}, \qquad \widetilde{\eta}_4 = \eta_4 \tag{32}$$

into system (28) yields

$$\begin{cases} \dot{\widetilde{\eta}} = \frac{1}{\varepsilon}G_0\widetilde{\eta} + Fv_2 + Fy_1 \\ y_2 = -c_0D(\varepsilon)\widetilde{\eta} \end{cases} \tag{33}$$

where $\widetilde{\eta} = [\widetilde{\eta}_1, \widetilde{\eta}_2, \widetilde{\eta}_3, \widetilde{\eta}_4]^T$, $D(\varepsilon) = \mathrm{diag}[\varepsilon, 1, \varepsilon, 1]$, and

$$G_0 = \begin{bmatrix} 0 & 1 & 0 & 0 \\ -a & -b & 0 & 0 \\ 0 & 0 & 0 & 1 \\ 0 & 0 & -a & -b \end{bmatrix}$$

$$u = \begin{bmatrix} \dfrac{A_{\delta_t^c} B_\alpha + \left(A_\alpha + \frac{a}{\varepsilon^2}\right) B_{\delta_t^c}}{A_{\delta_c^c} B_{\delta_t^c} - A_{\delta_t^c} B_{\delta_c^c}} & \dfrac{\frac{b}{\varepsilon} B_{\delta_t^c}}{A_{\delta_c^c} B_{\delta_t^c} - A_{\delta_t^c} B_{\delta_c^c}} & \dfrac{A_\omega B_{\delta_t^c} + \left(B_\omega + \frac{a}{\varepsilon^2}\right) A_{\delta_t^c}}{A_{\delta_c^c} B_{\delta_t^c} - A_{\delta_t^c} B_{\delta_c^c}} & \dfrac{\frac{b}{\varepsilon} A_{\delta_t^c}}{A_{\delta_c^c} B_{\delta_t^c} - A_{\delta_t^c} B_{\delta_c^c}} \\ \dfrac{A_{\delta_c^c} B_\alpha + \left(A_\alpha + \frac{a}{\varepsilon^2}\right) B_{\delta_c^c}}{A_{\delta_t^c} B_{\delta_c^c} - A_{\delta_c^c} B_{\delta_t^c}} & \dfrac{\frac{b}{\varepsilon} B_{\delta_c^c}}{A_{\delta_t^c} B_{\delta_c^c} - A_{\delta_c^c} B_{\delta_t^c}} & \dfrac{A_\omega B_{\delta_c^c} + \left(B_\omega + \frac{a}{\varepsilon^2}\right) A_{\delta_c^c}}{A_{\delta_t^c} B_{\delta_c^c} - A_{\delta_c^c} B_{\delta_t^c}} & \dfrac{\frac{b}{\varepsilon} A_{\delta_c^c}}{A_{\delta_t^c} B_{\delta_c^c} - A_{\delta_c^c} B_{\delta_t^c}} \end{bmatrix} \eta \triangleq P\eta. \tag{31}$$

Box I.

is a Hurwitz matrix. The derivative of Lyapunov function $V(\widetilde{\eta}) = \widetilde{\eta}^T P_0 \widetilde{\eta}$, where P_0 is the positive definite solution of the Lyapunov equation $P_0 G_0 + G_0^T P_0 = -I$, along the trajectories of system (33) is given by

$$\dot{V} = -\frac{1}{\varepsilon}\|\widetilde{\eta}\|^2 + 2\widetilde{\eta}^T P_0 F v_2 + 2\widetilde{\eta}^T P_0 F y_1. \tag{34}$$

Substituting the inequalities

$$\begin{cases} \widetilde{\eta}^T P_0 F v_2 \le \dfrac{1}{2}\|\widetilde{\eta}\|^2 + \dfrac{1}{2}\|F\|^2\|P_0\|^2\|v_2\|^2 \\ \widetilde{\eta}^T P_0 F y_1 \le \dfrac{1}{2}\|\widetilde{\eta}\|^2 + \dfrac{1}{2}\|F\|^2\|P_0\|^2\|y_1\|^2 \end{cases} \tag{35}$$

into Eq. (34), we obtain

$$\begin{aligned} \dot{V} \le & -\left(\frac{1}{\varepsilon} - 2\right)\|\widetilde{\eta}\|^2 + \|F\|^2\|P_0\|^2\|v_2\|^2 \\ & + \|F\|^2\|P_0\|^2\|y_1\|^2. \end{aligned} \tag{36}$$

We will always consider $\varepsilon < \frac{1}{2}$. Since

$$\lambda_{\min}(P_0)\|\widetilde{\eta}(t)\|^2 \le V(\widetilde{\eta}(t)) \le \lambda_{\max}(P_0)\|\widetilde{\eta}(t)\|^2 \tag{37}$$

we have

$$\begin{aligned} \|\widetilde{\eta}(t)\|^2 \le & \lambda_3 e^{-\lambda_1 t}\|\widetilde{\eta}(0)\|^2 + \frac{\lambda_2}{\lambda_1}(1 - e^{-\lambda_1 t}) \\ & \times \left(\sup_{0\le\tau\le t}\|y_1(\tau)\|^2 + \sup_{0\le\tau\le t}\|v_2(\tau)\|^2\right) \end{aligned} \tag{38}$$

and

$$\begin{aligned} |y_2(t)| \le & \|c_0\|\,\|D(\varepsilon)\widetilde{\eta}(t)\| \\ \le & \|c_0\|\,\|D(\varepsilon)\|\sqrt{\frac{\lambda_2}{\lambda_1}(1 - e^{-\lambda_1 t})}\sup_{0\le\tau\le t}\|v_2(\tau)\| \\ & + \|c_0\|\,\|D(\varepsilon)\|\sqrt{\frac{\lambda_2}{\lambda_1}(1 - e^{-\lambda_1 t})}\sup_{0\le\tau\le t}\|y_1(\tau)\| \\ & + \|c_0\|\sqrt{\lambda_3 e^{-\lambda_1 t}}\|\eta(0)\| \\ \triangleq & \gamma_2^v\left(\sup_{0\le\tau\le t}\|v_2(\tau)\|\right) + \gamma_2^y\left(\sup_{0\le\tau\le t}\|y_1\|\right) \\ & + \beta_2(\|\eta(0)\|, t) \end{aligned} \tag{39}$$

where $\lambda_1 = \left(\frac{1}{\varepsilon} - 2\right)\frac{1}{\lambda_{\max}(P_0)}$, $\lambda_2 = \frac{\|F\|^2\|P_0\|^2}{\lambda_{\min}(P_0)}$, and $\lambda_3 = \frac{\lambda_{\max}(P_0)}{\lambda_{\min}(P_0)}$. Due to the form of γ_2^y, there exists a constant $\varepsilon_0^* > 0$ such that Eq. (9) holds for $s_l = 0$ if $\varepsilon \le \varepsilon^* \triangleq \min\{\frac{1}{2}, \varepsilon_0^*\}$. In this case, due to Theorem 1, we have

$$\begin{aligned} \|y_2(t)\| \le & \beta_z(\|z(0)\|, t) + \gamma_{v1}\left(\sup_{0\le\tau\le t}|v_1(\tau)|\right) \\ & + \gamma_{v2}\left(\sup_{0\le\tau\le t}\|v_2(\tau)\|\right) + d_y^2 \end{aligned} \tag{40}$$

where $z = [\omega_q, \eta]^T$, γ_{v1} and γ_{v2} are class $\mathcal{K}$ functions, β_z is a class $\mathcal{KL}$ function, and d_y^2 is a nonnegative constant. It can be shown from Eqs. (29) and (40) that[2]

$$\begin{aligned} |\omega_q(t)| \le & \gamma'_{v1}\left(\sup_{0\le\tau\le t}|v_1(\tau)|\right) + \gamma'_{v2}\left(\sup_{0\le\tau\le t}\|v_2(\tau)\|\right) \\ & + \beta'_z(\|z(0)\|, t) + d_\omega \end{aligned} \tag{41}$$

holds for a pair of $\mathcal{K}$ functions $(\gamma'_{v1}, \gamma'_{v2})$, a class $\mathcal{KL}$ function β'_z, and a nonnegative constant d_ω. Therefore, by taking control law (31) with $\varepsilon \le \varepsilon^*$, system (27) is ISpS with respect to v_1 and v_2. □

Substituting Eq. (30) into Eq. (39) yields

$$\begin{aligned} |y_2(t)| \le & \gamma_2^v\left(\sup_{0\le\tau\le t}\|v_2(\tau)\|\right) + \gamma_2^y\left(\gamma_1^v\left(\sup_{0\le\tau\le t}|v_1(\tau)|\right) + \gamma_1^y\right. \\ & \left.\times\left(\sup_{0\le\tau\le t}|y_2(\tau)|\right) + \beta_1(|\omega_q(0)|, t) + d_y^1\right) \\ & + \beta_2(\|\eta(0)\|, t) \\ \le & \gamma_2^y \circ (Id + \rho_1) \circ \gamma_1^y\left(\sup_{0\le\tau\le t}|y_2(\tau)|\right) + \gamma_2^y \circ (Id + \rho_1^{-1}) \\ & \times\left(\gamma_1^v\left(\sup_{0\le\tau\le t}|v_1(\tau)|\right) + \beta_1(|\omega_q(0)|, t) + d_y^1\right) \\ & + \gamma_2^v\left(\sup_{0\le\tau\le t}\|v_2(\tau)\|\right) + \beta_2(\|\eta(0)\|, t). \end{aligned} \tag{42}$$

A fact to be noticed is that Eq. (9) implies the existence of a nonnegative real number d_0 such that

$$\begin{cases} \gamma_2^y \circ (Id + \rho_1) \circ \gamma_1^y(s) \le (Id + \rho_2)^{-1}(s) + d_0 \\ \gamma_1^y \circ (Id + \rho_2) \circ \gamma_2^y(s) \le (Id + \rho_1)^{-1}(s) + d_0 \end{cases}, \quad \forall s \ge 0$$

with $d_0 = 0$ if $s_l = 0$. Thus, Eq. (43) holds

$$\begin{aligned} |y_2(t)| \le & (Id + \rho_2)^{-1}\left(\sup_{0\le\tau\le t}|y_2(\tau)|\right) + d_0 + \gamma_2^y \circ (Id + \rho_1^{-1}) \\ & \times\left(\gamma_1^v\left(\sup_{0\le\tau\le t}|v_1(\tau)|\right) + \beta_1(|\omega_q(0)|, t) + d_y^1\right) \\ & + \gamma_2^v\left(\sup_{0\le\tau\le t}\|v_2(\tau)\|\right) + \beta_2(\|\eta(0)\|, t) \\ \le & (Id + \rho_2^{-1})\left(\beta_2(\|\eta(0)\|, t) + d_0 + \gamma_2^y \circ (Id + \rho_1^{-1})\right. \\ & \times\left(\gamma_1^v\left(\sup_{0\le\tau\le t}|v_1(\tau)|\right) + \beta_1(|\omega_q(0)|, t) + d_y^1\right) \\ & \left. + \gamma_2^v\left(\sup_{0\le\tau\le t}\|v_2(\tau)\|\right)\right). \end{aligned} \tag{43}$$

[2] For any class $\mathcal{K}$ function γ, any class $\mathcal{K}_\infty$ function ρ such that $\rho - Id$ is of class $\mathcal{K}_\infty$, and any nonnegative real numbers a and b we have

$\gamma(a + b) \le \gamma(\rho(a)) + \gamma(\rho \circ (\rho - Id)^{-1}(b))$.

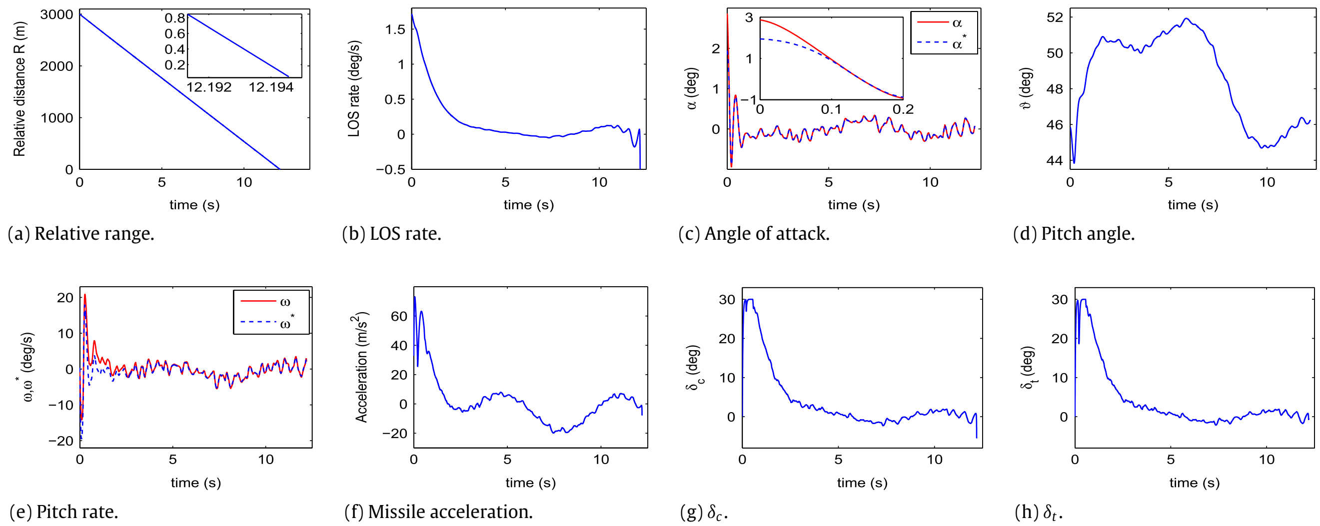

Fig. 2. The performance of the proposed IGC law in case 1.

Substituting Eq. (43) into Eq. (29) yields

$$\begin{aligned}|\omega_q(t)| \le{}& \alpha_0\left(\sup_{0\le\tau\le t}|v_1(\tau)|\right) + \alpha_0\Bigg((Id+\rho_2^{-1})\\ &\times\Bigg(\beta_2(\|\eta(0)\|,t) + d_0 + \gamma_2^v\left(\sup_{0\le\tau\le t}\|v_2(\tau)\|\right)\\ &+\gamma_2^y\circ(Id+\rho_1^{-1})\Bigg(\gamma_1^v\left(\sup_{0\le\tau\le t}|v_1(\tau)|\right)\\ &+\beta_1(|\omega_q(0)|,t)+d_y^1\Bigg)\Bigg)\Bigg) + \beta_0(|\omega_q(0)|,t).\end{aligned} \tag{44}$$

Since $d_0 = 0$ holds for $0 < \varepsilon \le \varepsilon^*$, and $\gamma_2^v, \gamma_2^y \to 0$ as $\varepsilon \to 0$, it can be seen that the right-hand side of (44) approaches

$$\alpha_0\left(\sup_{0\le\tau\le t}|v_1(\tau)|\right) + \alpha_0\circ(Id+\rho_2^{-1})(\beta_2(\|\eta(0)\|,t)) + \beta_0(|\omega_q(0)|,t).$$

as $\varepsilon \to 0$ for bounded v_1, v_2 and d_y^1, which shows that for sufficiently small ε the influence of v_2 and d_y^1 on ω_q will be close to zero. Besides that, since $\alpha_0(x) = \frac{\xi}{\sqrt{2KR_m}}\sqrt{1-e^{-2Kt}}x$, v_1 can be suppressed by adjusting ξ and K.

According to Theorem 3 and Eq. (23), the IGC law can be written as

$$\begin{bmatrix}\delta_c^c\\ \delta_t^c\end{bmatrix} = E\begin{bmatrix}\delta_c\\ \delta_t\end{bmatrix} + P\eta. \tag{45}$$

Remark 2. The form of term $P\eta$ is similar to a PD controller, which aims at providing a sufficiently fast tracking of the command profiles to guarantee stability of the integrated system.

4. Simulation results

This section presents simulation results for the closed-loop system with the proposed IGC law (45). In this simulation study the constant missile speed is assumed to be $V_M = 380\ \mathrm{m/s^2}$. The missile model parameters are $l_\alpha = 800\ \mathrm{m/s^2}$, $l_{\delta_c} = l_{\delta_t} = 60\ \mathrm{m/s^2}$, $m_\alpha = -100\ \mathrm{s^{-2}}$, $m_\omega = -5\ \mathrm{s^{-1}}$, $m_{\delta_c} = 50\ \mathrm{s^{-2}}$, $m_{\delta_t} = -50\ \mathrm{s^{-2}}$, and $\tau_c = \tau_t = 0.03\ \mathrm{s^{-1}}$. The initial missile attitude and control fins are $\alpha(0) = 0.05$ rad, $\vartheta(0) = 0.8$ rad, $\omega(0) = 0$, and $\delta_c(0) = \delta_t(0) = 0$. The actuator commands are assumed to be limited by $|\delta_c| \le \frac{\pi}{6}$, $|\delta_t| \le \frac{\pi}{6}$, and the maximum missile acceleration is $a_M^{\max} = 100\ \mathrm{m/s^2}$. The initial variables of relative motion are $R(0) = 3000$ m and $q(0) = \frac{\pi}{4}$. The initial target speed and fight path angle are $V_T = 200$ m/s and $\varphi_T(0) = 1.32$ rad. It is easy to calculate the initial LOS rate, $\omega_q(0) = 0.03$ rad/s. Here, we define the command profile α^* to be a hyperbolic tangent function $\alpha^* = 0.04\tanh(\alpha/0.04) = 0.04\frac{e^{\alpha/0.04}-e^{-\alpha/0.04}}{e^{\alpha/0.04}+e^{-\alpha/0.04}}$, which is a smooth function bounded by 0.04 rad. The LOS rate is taken as a first-order lag system with a time constant 0.005 s with the additive Gaussian noise with mean zero and standard deviation 0.1 mrad, and other feedback states are taken with the same noise as well. Uncertainties Δ_α and Δ_ω are set as $\Delta_\alpha = 0.03\sin(t)$ rad/s $+ \Delta_\alpha^r$, $\Delta_\omega = 0.3\cos(t)\ \mathrm{rad/s^2} + \Delta_\omega^r$, where Δ_α^r and Δ_ω^r are random uncertainties of Gaussian noises with deviations of 0.01 rad/s and 0.2 $\mathrm{rad/s^2}$, respectively. The contribution of gravity to lift of $\frac{g\cos(\vartheta-\alpha)}{V_M}$ is also taken into consideration in the simulation. Because the angles using 'radian' may seem to be small but the actual angle may be large, the unit of 'degree' is used in all the simulation figures related to angles.

Case 1: Suppose that the target does not maneuver. The guidance and control coefficients are chosen as $K = 5$, $\xi = 1$, $\varepsilon = 0.01$, and $a = b = 1$. The simulation results are shown in Fig. 2. Fig. 2(a) and (b) give curves of the target-to-missile range and LOS rate. When homing guidance begins, ω_q rapidly converges to a small neighborhood of zero. The miss distance is only about $R = 0.05$ m, which means a successful interception. The response of missile dynamics during the process of homing guidance is shown in Fig. 2(c)–(f). At the beginning of the homing guidance, the missile acceleration is relative large so as to adjust flight direction to nullify LOS rate, and when LOS rate converges to a very small value, missile acceleration together with angle of attack and pitch rate is kept around zero. Fig. 2(g) and (h) illustrate canard and tail deflections.

Case 2: Assume that the target escapes with acceleration of $a_{T_q} = 60\cos(\frac{\pi}{3}t)\ \mathrm{m/s^2}$. The guidance and control coefficients are chosen as $K = 1$, $\xi = 0.1$, $\varepsilon = 0.01$, and $a = b = 1$. The simulation results are shown in Fig. 3. From Fig. 3(a) and (b) we can see that, when homing guidance begins, ω_q rapidly converges to a small neighborhood of zero, and can be kept near zero although the target normal acceleration always exists, until the range R decreases to an extremely small value ($R \approx 0.05$ m). Compared with Fig. 2(b), the deviation of LOS rate from zero is a little larger due to target maneuvers, but a successful interception can also be

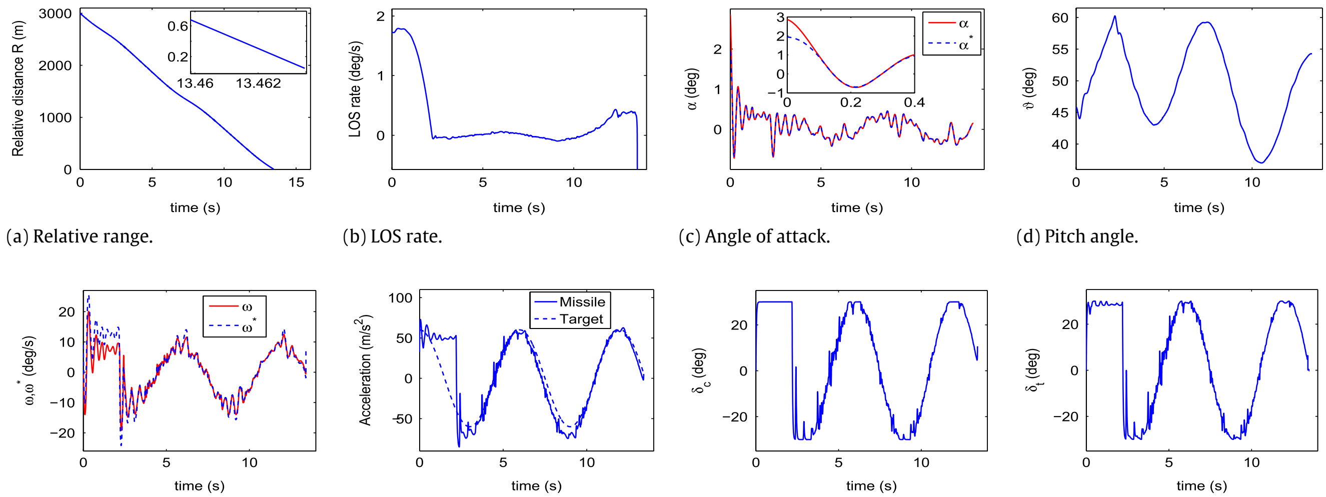

(a) Relative range. (b) LOS rate. (c) Angle of attack. (d) Pitch angle.

(e) Pitch rate. (f) Missile acceleration. (g) δ_c. (h) δ_t.

Fig. 3. The performance of the proposed IGC law in case 1.

obtained, which is verified by Fig. 3(a). Fig. 3(c)–(f) depicts the response of missile dynamics of case 2. The angle of attack and the pitch rate can track their commands rapidly, which guarantees that the missile can generate an expected acceleration to intercept the target. Either α or ω is kept in a reasonable domain in the whole process of this simulation. The missile acceleration is shown and compared with the target acceleration in Fig. 3(f). Finally, Fig. 2(g) and (h) illustrate canard and tail deflections.

5. Conclusions

An integrated guidance and control (IGC) law is designed in this paper based on small-gain theorem for missiles steered by both canard and tail controls. The developed approach, when compared with the existing results, is novel in that the IGC law can guarantee stability of the overall system including the guidance and control loop without the assumption that the angle between LOS and missile velocity is almost invariable. It is shown that the line-of-sight (LOS) rate under the IGC law is input-to-state practically stable (ISpS) with respect to target maneuvers and missile model uncertainties. Simulation results have confirmed the effectiveness of the proposed scheme on intercepting maneuvering targets and guaranteeing the stability of missile dynamics.

Appendix. Derivation of Eq. (18)

$$\begin{aligned}\dot{a}_M^* &= \frac{\sin(q-\varphi_M)}{\cos^2(q-\varphi_M)}(q-\dot{\varphi}_M)\Gamma\omega_q + \frac{\omega_q}{\cos(q-\varphi_M)}\\ &\quad\times\left(\left(K+\frac{1}{2\xi^2}\right)V_R - 2\dot{V}_R\right) + \frac{\Gamma\dot{\omega}_q}{\cos(q-\varphi_M)} \end{aligned} \tag{A.1}$$

$$\begin{aligned}\dot{V}_R &= a_{T_R} - \sin(q-\varphi_M)V_M\dot{\varphi}_M\\ &\quad + V_M\sin(q-\varphi_M)\omega_q - V_T\sin(q-\varphi_T)\omega_q \end{aligned} \tag{A.2}$$

where $\Gamma = R(K+\frac{1}{2\xi^2}) - 2V_R$, $a_{T_R} = \dot{V}_T\cos(q-\varphi_T) + V_T\sin(q-\varphi_T)\dot{\varphi}_T$. By applying Eqs. (1)–(3) and (A.2) into Eqs. (18) and (A.1) can be obtained.

References

Idan, M., Shima, T., & Golan, O. M. (2007). Integrated sliding mode autopilot-guidance for dual-control missiles. *Journal of Guidance Control and Dynamics*, *30*(4), 1081–1089.

Jiang, Z. P., Teel, A. R., & Praly, L. (1994). Small-gain theorem for ISS systems and applications. *Mathematics of Control, Signals, and Systems*, *7*(2), 95–120.

Menon, P. K., & Ohlmeyer, E. J. (1999). Integrated design of agile missile guidance and control systems. In *Proceedings of the 7th Mediterranean conference on control and automation*. Haifa (pp. 1469–1494).

Menon, P. K., & Ohlmeyer, E. J. (2001). Integrated design of agile missile guidance and autopilot systems. *Control Engineering Practice*, *9*(10), 1095–1106.

Palumbo, N. F., & Jackson, T. D. (1999). Integrated missile guidance and control: a state dependent Riccati differential equation approach. In *Proceedings of international conference on control applications*. Hawai'i (pp. 243–248).

Sharma, M., & Richards, N. D. (2004). Adaptive, integrated guidance and control for missile interceptors. *AIAA paper 2004-4880*.

Shima, T., Idan, M., & Golan, O. M. (2006). Sliding-mode control for integrated missile autopilot guidance. *Journal of Guidance Control and Dynamics*, *29*(2), 250–260.

Shtessel, Y. B., Shkolnikov, I. A., & Levant, A. (2007). Smooth second-order sliding modes: missile guidance application. *Automatica*, *43*(8), 1470–1476.

Shtessel, Y. B., Shkolnikov, I. A., & Levant, A. (2009). Guidance and control of missile interceptor using second-order sliding modes. *IEEE Transactions on Aerospace and Electronic Systems*, *45*(1), 110–124.

Shtessel, Y. B., & Tournes, C. (2009). Integrated higher-order sliding mode guidance and autopilot for dual-control missiles. *Journal of Guidance, Control, and Dynamics*, *45*(2), 110–124.

Sontag, E. D. (1989). Smooth stabilization implies coprime factorization. *IEEE Transactions on Automatic Control*, *34*(4), 435–443.

Tournes, C., & Wilkerson, P. (2001). Integrated terminal guidance and automatic pilot using subspace-stabilization. *AIAA paper 2001-4275*.

Williams, D. E., Richman, J., & Friedland, B. (1983). Design of an integrated strapdown guidance and control system for a tactical missile. *AIAA paper 1983-2169*.

Wise, K. A., & Broy, D. J. (1998). Agile missile dynamics and control. *Journal of Guidance, Control, and Dynamics*, *21*(3), 441–449.

Xin, M., Balakrishnan, S. N., & Ohlmeyer, E. J. (2006). Integrated guidance and control of missiles with θ-D method. *IEEE Transactions on Control Systems Technology*, *14*(6), 981–992.

Yang, C. D., & Yang, C. C. (1997). A unified approach to proportional navigation. *IEEE Transactions on Aerospace and Electronic Systems*, *33*(2), 557–567.

Zhou, D., Sun, S., & Teo, K. L. (2009). Guidance laws with finite time convergence. *Journal of Guidance, Control, and Dynamics*, *32*(6), 1838–1846.

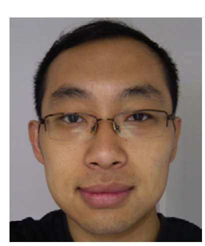

Han Yan was born in Changchun, China, in 1985. He received the B.Eng. degree in Automation from University of Science and Technology of China in 2008. He is currently a Ph.D. Candidate in Department of Automation, University of Science and Technology of China, Hefei, China. His research interests include nonlinear and control theories, and their applications to the missile guidance and control.

Haibo Ji was born in Anhui, China, in 1964. He received the B.Eng. degree and Ph.D. degree in Mechanical Engineering from Zhejiang University and Beijing University, in 1984 and 1990, respectively. He is currently a Professor in Department of Automation, University of Science and Technology of China, Hefei, China. His research interests include nonlinear control and adaptive control, and their applications.